SCIENCE CHINA
Earth Sciences

• RESEARCH PAPER •

September 2012 Vol.55 No.9: 1504–1517
doi: 10.1007/s11430-012-4422-3

Numerical simulation study of temperature change over East China in the past millennium

XIAO Dong[1], ZHOU XiuJi[1,2*] & ZHAO Ping[3]

[1] *Chinese Academy of Meteorological Sciences, Beijing 100081, China;*
[2] *State Key Laboratory of Severe Weather, Beijing 100081, China;*
[3] *National Meteorological Information Centre, Beijing 100081, China*

Received May 4, 2011; accepted November 28, 2011; published online May 10, 2012

Despite many studies on reconstructing the climate changes over the last millennium in China, the cause of the China's climate change remains unclear. We used the UVic Earth System Climate Model (UVic Model), an Earth system model of intermediate complexity, to investigate the contributions of climate forcings (e.g. solar insolation variability, anomalous volcanic aerosols, greenhouse gas, solar orbital change, land cover changes, and anthropogenic sulfate aerosols) to surface air temperature over East China in the past millennium. The simulation of the UVic Model could reproduce the three main characteristic periods (e.g. the Medieval Warm Period (MWP), the Little Ice Age (LIA), and the 20th Century Warming Period (20CWP)) of the northern hemisphere and East China, which were consistent with the corresponding reconstructed air temperatures at century scales. The simulation result reflected that the air temperature anomalies of East China were larger than those of the global air temperature during the MWP and the first half of 20CWP and were lower than those during the LIA. The surface air temperature of East China over the past millennium has been divided into three periods in the MWP, four in the LIA, and one in the 20CWP. The MWP of East China was caused primarily by solar insolation and secondarily by volcanic aerosols. The variation of the LIA was dominated by the individual sizes of the contribution of solar insolation variability, greenhouse gas, and volcano aerosols. Greenhouse gas and volcano aerosols were the main forcings of the third and fourth periods of the LIA, respectively. We examined the nonlinear responses among the natural and anthropogenic forcings in terms of surface air temperature over East China. The nonlinear responses between the solar orbit change and anomalous volcano aerosols and those between the greenhouse gases and land cover change (or anthropogenic sulfate aerosols) all contributed approximately 0.2°C by the end of 20th century. However, the output of the energy-moisture balance atmospheric model from UVic showed no obvious nonlinear responses between anthropogenic and natural forcings. The nonlinear responses among all the climate forcings (both anthropogenic and natural forcings) contributed to a temperature increase of approximately 0.27°C at the end of the 20th century, accounting for approximately half of the warming during this period; the remainder was due to the climate forcings themselves.

past millennium, East China, climate forcings, UVic Model, nonlinear response

Citation: Xiao D, Zhou X J, Zhao P. Numerical simulation study of temperature change over East China in the past millennium. Sci China Earth Sci, 2012, 55: 1504–1517, doi: 10.1007/s11430-012-4422-3

The International Panel of Climate Change (IPCC) Fourth Assessment Report proposed that the average air temperature in the second half of the 20th century may be higher than the mean for any 50-a period in the past 1300 years [1]. This view has attracted worldwide attention. However, the Earth's climate has experienced cool-warm and dry-wet natural variations and warmer conditions than those in the 20th century. It is still an open question whether anthropogenic activities are entirely responsible for the warming of

*Corresponding author (email: xjzhou@cams.cma.gov.cn)

the 20th century or whether natural variability makes significant contributions. Hence, it is necessary to investigate the climate changes over the past millennium to understand the causes and mechanisms of the climate change in the past century [2].

The global mean temperature has been recorded by instruments since 1850. Therefore, to understand the climate before then, it is necessary to employ the proxy data. Mann et al. [3, 4] reconstructed the temperature over the past 600 years and then extended it to the past millennium. When plotted, the temperature time series, which declined slowly until it ascended since the 20th century, is analogous to a hockey stick. The debate over the hockey-stick pattern has been ongoing since its inception. Soon et al. [5] indicated that there was a Mediaeval Warm Period (MWP) from 800 to 1300 AD and a Little Ice Age (LIA) from 1300 to 1900 AD. The time series of air temperatures in the past millennium produces a graph more similar to a wet noodle than to a hockey stick. Recently, Jones and Mann et al. [6–8] published several time series of air temperatures, which show the existence of the MWP and LIA. The LIA of China is very clear. It has been debated whether the MWP existed in East China. It has also been demonstrated that the MWP in East China was distinct and warmer than that in West China [9].

Many studies have reconstructed the air temperature and precipitation over China. For example, Wang et al. [10], who reconstructed 30 time series of air temperatures worldwide with a time resolution of 25 years, evaluated the homogeneity and reliability of proxy data by Mann, Jones, Crowley and Briffa and established the air temperatures for ten regions in China in the past millennium, with a time resolution of 10 years [11]. Yang et al. [12] contributed a time series of air temperatures over China during the past two millennia according to proxy data from tree rings, ice cores, historical records, and other sources. Ge et al. [13] presented a wintertime air temperature time series over the middle and lower reaches of the Yangtze River over the past two millennia. Tan et al. [14] reconstructed a 2650-a time series for warm season (May–August) air temperature in Beijing, whose cold-warm alternations generally correspond to the vicissitudes of dynasties. Shao et al. [15] established a precipitation index of the Delingha region for the past two millennia. Yao et al. [16] presented a two-thousand-year air temperature series based on the Guliya ice core. Furthermore, Wang et al. [9, 10, 17], Chu and Ren [18], Zheng and Wang [19], and Zhou et al. [2] introduced domestic and foreign climate research for the past millennium, which has been instrumental to the development of millenary climate research in China.

The above efforts have contributed greatly to elucidating the features of China's climate over the past millennium. However, the numerical simulations and data analyses have not been adequate to determine the causes of climate changes. Wang et al. [10] simulated the climate change over the past millennium using a zero-dimensional energy balance model, defining the main low frequency variation. Liu et al. [20, 21] simulated the climate change over China in the past millennium under the combined forcings of solar activity, volcanic activity, and greenhouse gases using the Germanic ECHO-G Model and displayed the features and causes of three characteristics epochs. Zhang et al. [22] and Man et al. [23] simulated the climate characteristics of LIA using the FGOALS_gl Model. Zhou and Yu [24] ran the FGOALS_gl Model to examine the warming of the 20th century. At present, numerical simulations of the climate change over the past millennium are still scarce, especially simulations under individual forcings, such as solar insolation, volcanic aerosols, greenhouse gases, solar orbit change, and the recent arresting land cover change and sulfate aerosols. Transient simulations of individual climate forcing factors are conducive to disclosing their contributions to climate change. This paper aims to investigate the individual and total contributions of the above climate forcing factors to the climate change of East China and the nonlinear responses among them (including between the natural and anthropogenic factors). The temperature of East China is represented by the averaged temperature over the region (100°–120°E, 20°–45°N) unless otherwise stated.

1 Model and data

Generally, equilibrium and transient experiments are employed to explore scientific problems in paleoclimatological numerical studies. The climate forcings in the equilibrium experiment are set to the mean values during that period, and they fluctuate over time in the transient experiment. The advantages of the equilibrium experiments are that they are less influenced by inner variability, are easier to compare with one another, and can better explain the physical mechanism. Transient experiments can disclose the response of the climate system to the climate forcings and examine the contribution of climate forcing to the climate change during the period. There are also some differences between these two kinds of experiments [25]. To examine the contribution of climate forcing to the temperature change of East China, it is necessary to run the transient experiments under individual forcings.

A vast amount of computer time is required to run transient experiments under individual forcings by employing the General Coupled Ocean-Atmosphere Model. However, the Energy Balance Model (EBM) is useful only for the study of mechanism because the EBM does not contain the inner process of the climate system and cannot show the spatial distribution. Also, the physical process contained in the EBM is too simple [2]. Therefore, we employed an Earth system model of intermediate complexity, the UVic Earth System Climate Model (UVic Model), which was generally able to describe the nonlinear response among the components of the climate system and show the spatial dis-

tribution [25]. The averaged error of air temperature simulated by the UVic Model was even smaller than that by some of the famous complex models [26].

The UVic Model was released by the University of Victoria, Canada. This model couples atmospheric, oceanic, sea ice, land surface, and vegetation models. The atmosphere model comprises a single layer: a vertically integrated energy-moisture balance model. Version 2.2 of the GFDL Modular Ocean Model, with 19 vertical levels, is employed as the ocean component of the UVic Model. The land surface model is the MOSES model (Met Office Surface Exchange Scheme). The TRIFFID model (Top-down Representation of Interactive Foliage and Flora Including Dynamics) of the Hadley Center is coupled as a vegetation model. The resolution of this coupled model is 3.6° longitude and 1.8° latitude. The UVic Model is used widely in paleoclimate, modern climate, and future climate studies [26–29].

The transient forcings are shown in Figure 1. The solar insolation variability [30, 31], relative to 1365 W m^{-2}, presents three episodes: it is stronger in 1000–1420 and 1600–2000 and weaker in 1420–1600. The second panel in the figure shows anomalous volcanic aerosol forcings relative to the mean values for 1600–1990 [32, 33]. The additional greenhouse gas forcing (i.e. non-CO_2 greenhouse gases) varied from 0 W m^{-2} in 1850 to 0.8 W m^{-2} in 2000 (Figure 1(c)), and the northern hemispheric (NH) average optical depth of anthropogenic sulfate aerosol increased from 0 in 1850 to 0.035 in 2000 [27] (Figure 1(d), right side). The CO_2 concentrations were less than 280 ppmv during 1585–1785 but increased in the following 200 years to 369 ppmv at the end of the 20th century [34] (Figure 1(d), left side). Global land cover changes during the past 300 years have also been taken into account. Based on the zonal mean data presented by Bauer et al. [35], land cover change in the NH midlatitude affected an area of 0.5×10^6 km^2 from 1500–1700, an order of magnitude less than that after 1700. Therefore, for the period prior to 1700, we used land cover change data for the year 1700.

Climate forcings were divided into two categories: (1) natural forcings (volcanic aerosols (Volcano), solar insolation variability (Solar), and solar orbital changes (Orbit)) and (2) anthropogenic forcings (historical land-cover change (LCC), greenhouse gases (GG), and anthropogenic sulfate aerosols (Sulfate)). The greenhouse gases were considered both CO_2 and non-CO_2 in this model. Other non-CO_2 greenhouse gases are referred to as additional greenhouse gas (AGG). It is noted that CO_2 could be considered a natural climate forcing factor before industrialization and an anthropogenic climate forcing factor after industrialization (1750 AD). CO_2 is considered an anthropogenic climate forcing factor in this paper.

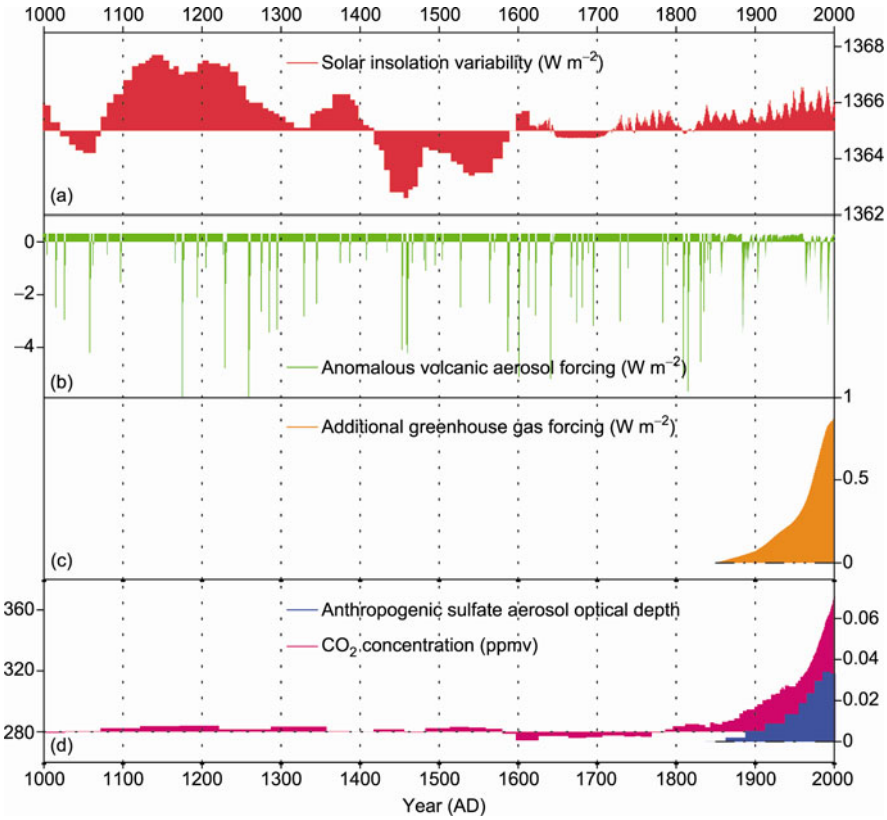

Figure 1 Time series of climate forcing factors: solar insolation variability, anomalous volcano aerosol forcing, additional greenhouse gas forcing, CO_2 concentration and NH average optical depth of anthropogenic sulfate aerosol.

A control equilibrium was spun up for 2000 years using year 1000 conditions (solar constant, land cover change, and orbital parameters), with greenhouse gases set to 280 ppmv, anomalous volcanic aerosols set to 0.31 W m^{-2} (mean values for 1600–1990), and sulfate aerosols set to zero (Table 1). Each transient scenario was run from the year 1000 to the year 1999. The transient effects for climate forcings were considered in scenarios of individual forcing (Volcano, Solar, Orbit, GG, Sulfate, LCC); combinations of all model forcings (ALL); anthropogenic forcings (ANTH) only; natural forcings (NAT) only; individual pairs of anthropogenic forcings; and individual pairs of natural forcings. The abbreviations of climate forcings (as defined above) are mainly used in the figure captions and descriptions.

The contribution of climate forcings to the variation of surface air temperature of East China is defined as the East China surface air temperature of the climate forcings transient run minus that of the equilibrium run, which represents the contribution of this climate forcing to the climate variation. Nonlinear responses among the climate forcings are defined as the contribution of the combined climate forcings minus the linear sum of the contributions of individual climate forcings. The contributions and nonlinear responses are all toward the surface air temperature of East China, unless stated otherwise.

2 NH and East China temperature simulated by the UVic Model

2.1 Comparison between the simulated and reconstructed NH temperature

Figure 2 shows the 11-a moving mean NH surface air temperature (red line) simulated by the UVic Model under all forcings. The figure presents a warm period during 1000–1430 AD and a cold period from 1430 to 1900, viz., the MWP and LIA, respectively. The warm period from 1900 to the present is called the 20th Century Warm Period (20CWP). The UVic Model was able to reproduce the three characteristic periods of NH surface air temperature in the past millennium, namely, the MWP, the LIA, and the 20CWP.

A comparison of the simulated NH surface air temperature with the reconstructed temperature by Mann et al. [8] (M08) shows an opposite tendency between the UVic and M08 before 1180 AD. UVic was approximately 0.2°C warmer than M08 during 1180–1260, and both had a concurrent tendency. The value of the temperature of UVic was

Table 1 List of numerical simulated experiments[a)]

Experiment titles	Period of time	Values of the climate forcing factor						
		Solar insolation	Solar orbit parameter	Anomalous volcanic aerosols	Land cover change	CO_2	Additional greenhouse gas	Sulfate aerosols
Equilibrium (Equ)	1000–1999	1366 W m^{-2}	Parameters of 1000AD	0.31 W m^{-2}	Data of 1700 AD	280 ppmv	0	0
All forcings (All)	1000–1999	T	T	T	T	T	T	T
Solar insolation (Solar)	1000–1999	T	–	–	–	–	–	–
Solar orbit (Orbit)	1000–1999	–	T	–	–	–	–	–
Anomalous volcanic aerosols (Volcano)	1000–1999	–	–	T	–	–	–	–
Land cover change (LCC)	1000–1999	–	–	–	T	–	–	–
Greenhouse gas (GG)	1000–1999	–	–	–	–	T	T	–
CO_2 (CO_2)	1000–1999	–	–	–	–	T	–	–
Additional greenhouse gas (AGG)	1000–1999	–	–	–	–	–	T	–
Sulfate aerosols (Sulfate)	1000–1999	–	–	–	–	–	–	T
Natural forcings (Nat)	1000–1999	T	T	T	–	–	–	–
Anthropogenic forcings (Anth)	1000–1999	–	–	–	T	T	T	T
Solar+Orbit	1000–1999	T	T	–	–	–	–	–
Orbit+Volcano	1000–1999	–	T	T	–	–	–	–
Volcano+Solar	1000–1999	T	–	T	–	–	–	–
GG+LCC	1000–1999	–	–	–	T	T	T	–
LCC+Sulfate	1000–1999	–	–	–	T	–	–	T
Sulfate+GG	1000–1999	–	–	–	–	T	T	T
CO_2+LCC	1000–1999	–	–	–	T	T	–	–
CO_2+Sulfate	1000–1999	–	–	–	–	T	–	T
Agg+LCC	1000–1999	–	–	–	T	–	T	–
Agg+Sulfate	1000–1999	–	–	–	–	–	T	T

a) The values of climate forcings in the control run (Equ) are set to that of 1000 AD. The data of land cover change before 1700 AD were adapted to the data of 1700 AD because the value of land cover change before 1700 AD is smaller than that after 1700 AD. The line (–) indicates that this forcing is not included in this experiment. The letter "T" denotes that this forcing was included and fluctuated over time in this transient experiment.

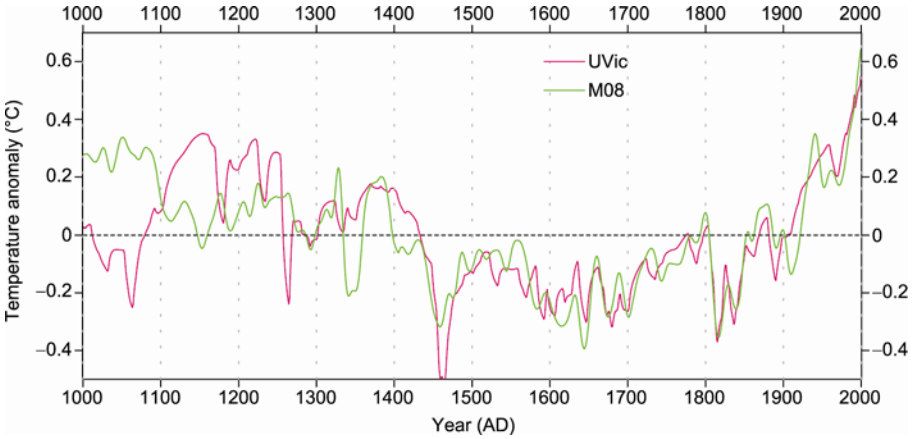

Figure 2 Comparison between the simulated NH surface air temperature (UVic) and M08 [8]. The two time series are both anomalies relative to their individual millennial mean.

roughly analogous to that of M08 during 1260–1430. The values and tendencies of UVic and M08 were in good agreement in the LIA and 20CWP. The increase in UVic and M08 values reached approximately 0.6°C by the end of the 20th century.

The correlation coefficient of the NH temperature between UVic and M08 is 0.6 during 1000-1999 and is significant at the 99.9% confidence level (Table 2). We noted the opposite tendency between UVic and M08 before 1180 AD. However, the correlation coefficient during 1181–1999 between them is 0.76, and between the 11-a moving mean time series is 0.85 (Table 2), respectively. The effective free degrees of the time series of the 11-a moving mean NH temperature of UVic and M08 during 1181–1999 decreased to 31 [36]. However, the correlation coefficients are still significant at the 99.9% confidence level. The simulated NH surface air temperature was in good agreement with the reconstructed M08 after 1180. Generally, the NH surface air temperature simulated by the UVic Model could reproduce three characteristic periods and their individual century-scale variations in the past millennium.

Table 2 Correlation coefficients between simulated and reconstructed NH surface air temperature in several periods[a)]

Correlation coefficient	M08		
	1000–1850	1000–1999	1181–1999
UVic	0.51	0.60	0.76
UVic11	0.57	0.65	0.85

a) UVic and UVic11 represent the simulated surface air temperature by the UVic Model and the 11-a moving mean simulated surface air temperature. All the correlation coefficients are significant at the 0.001 confidence level.

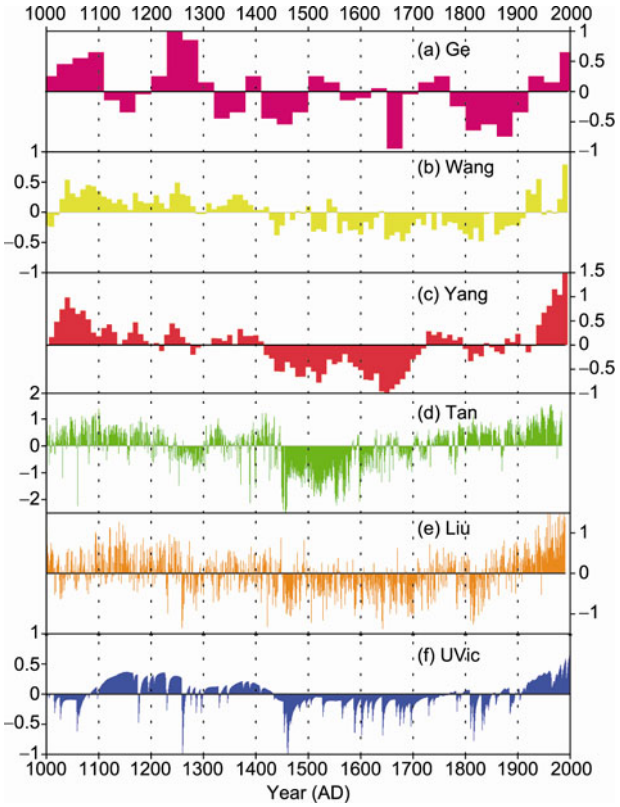

Figure 3 Comparison among the simulated and reconstructed air temperatures of East China in the past millennium. (a) Winter temperature of East China (Ge, the surname of data contributor for short); (b) annual temperature of East China (Wang); (c) annual temperature of China (Yang); (d) warm season (May-Aug) temperature of Beijing (Tan); (e) ECHO-G model simulated temperature of East China (Liu); and (f) UVic simulated temperature of East China (UVic). All time series were anomalies relative to the individual millennial mean. Unit: °C.

2.2 Comparison between the simulated and reconstructed East China temperature

Figure 3(a) shows the winter temperature of East China reconstructed by Ge et al. [13]. There are three warm periods during 1000–1125, 1200–1290, and 1980–2000 and one cold period for the remaining time. Figure 3b shows the annual mean temperatures of East China as reconstructed by Wang et al. [11] for the MWP during 1030–1430, the LIA during 1430–1910, and the 20CWP from 1920 to the pre-

sent. The MWP can also be divided into three periods of 1030–1150, 1160–1280, and 1290–1420. The reconstructed temperature of China (Figure 3(c)) by Yang et al. [12] indicated that the periods of the MWP, LIA, and 20CWP were 1420–1930, 1420–1930, and 1920 to the present, respectively. Their LIA had two different stages: 1420–1720 and 1730–1930. The first stage was 0.5°C warmer than the second. The temperature of the Beijing warm season (Figure 3d) reconstructed by Tan et al. [14] shows the MWP during 1000–1450, a short LIA during 1450–1700, and the 20CWP after 1700. The annual temperature of East China (Figure 3(e)) simulated by the ECHO-G model displays the MWP during 1000–1450, the LIA during 1450–1850, and the 20CWP from 1850 to the present. The temperature anomalies at the end of the 20th century had reached 1.5°C, which is warmer than the observed. Figure 3(f) shows the temperature anomalies of East China with the MWP during 1000–1430, the LIA during 1430–1900, and the 20CWP during 1000–1999.

There are obvious MWP and LIA patterns in the summer, winter and annual temperatures of East China, although their durations are different. The duration of the LIA in summer (1430–1700) is shorter than that in winter (1320–1920). Furthermore, the correlation coefficient between winter (Figure 3(a)) and summer (Figure 3(d)) temperatures in East China is close to zero, and neither had a significant correlation with annual temperature (Table 3). The annual mean temperature of East China simulated by the UVic Model is in good agreement with the variation of temperature by Yang et al. (Figure 3(c)) and Wang et al. (Figure 3(b)) and with the starting and finishing time of the MWP and LIA. The correlation coefficients between the temperature of the UVic Model and the reconstructed temperature by Wang and Yang are 0.52 and 0.5, respectively (Table 3). For the temperature of the ECHO-G Model, the correlation coefficients are 0.48 and 0.67, respectively. However, the correlation coefficient between the temperature of East China in the UVic Model and the reconstructed temperature of East China by Wang is higher than the others. Therefore, the UVic Model could reproduce the variation in the temperature over East China well.

It can be seen from the above comparisons that the UVic Model could reproduce the main low-frequency variations and even the century scale variations of the temperature of either the NH or East China. The correlation coefficients between the NH (East China) temperature of the UVic Model and that reconstructed by Mann (Wang) et al. are 0.85 (0.5) and are significant at the 99.9% confidence level. Therefore, it is feasible to employ the UVic Model to understand the century-scale temperature changes of NH and East China in the past millennium.

3 Spatial distribution of temperature variation of East China and its relation to global temperature

To understand the spatial distribution of the temperature over East China and its uniqueness, it is necessary to compare it to the global distribution. Figure 4 shows the epochal differences among the MWP, LIA and 20CWP. Compared with the typical epoch of the MWP (1100–1260) and LIA (1600–1700), the temperature of the MWP is warmer globally than that of the LIA, except for the Weddell Sea (Figure 4(a)). The differences in Figure 4(a) exceed 0.3°C to the north of 30°S, 0.5°C over the North Pole, 0.45°C over East China, and 0.4°C over West China. The temperature of East China was warmer than that of West China, which is in accordance with the result of the reconstructed data. The differences between the typical epoch of the 20CWP (1950–1999) and that of the LIA (1600–1700) presented 0.8°C over the Warm Pool, 0.6°C over the North Pole, 0.5–0.65°C over China (larger in South China), and 0.4°C over Europe (Figure 4(b)). Compared with the MWP, the 20CWP is 0.3°C warmer over the Warm Pool and the South Pole and 0.05°C cooler over the East Europe-Ural Mountains (Figure 4(c)). Crowley and Lowery [37] noted that the temperature of some European stations in the MWP was warmer than that in the 20CWP. Mann et al. [38] compared the spatial differences between the surface air temperature of the MWP and 20CWP. The result indicated that the temperatures of the MWP over the North Atlantic, northern Europe, the

Table 3 Correlation coefficients between pairs of simulated or reconstructed air temperatures of East China[a)]

Correlation coefficients	Wang	Tan	Ge	Yang	Liu	UVic
	1000–1990, 10, 100	1000–1985, 1, 986	1005–1995, 30, 33	1000–2000, 10, 101	1000–1990, 1, 991	1000–1999, 1, 1000
Wang		0.3	0.3	0.64	0.48	0.5
Tan			0.04	0.63	0.38	0.38
Ge				0.31	0.36	–0.15
Yang					0.67	0.52
Liu						0.61

a) The numbers in the second row represent the period, resolution and samples of the data. To calculate the correlation coefficient between the data with different resolutions, the high-resolution data were interpolated into the low-resolution data. The shaded correlation coefficients are significant at a 0.001 confidence level, except the correlation coefficient between Wang and Tan, which is significant at the 0.01 confidence level. The non-shaded coefficients do not exceed the 0.05 confidence level.

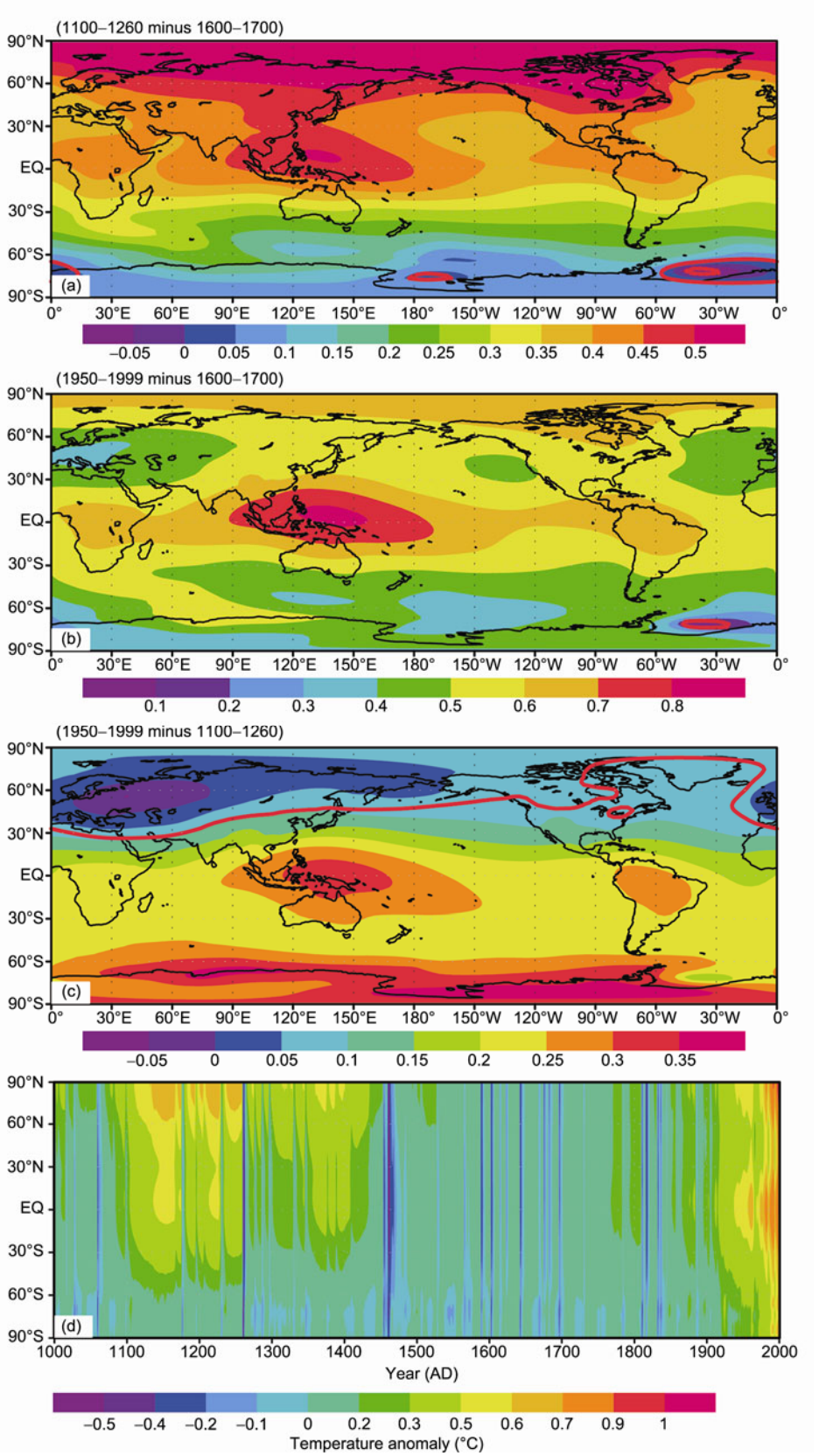

Figure 4 (a) Differences of surface air temperature between the LIA and MWP; (b) differences of surface air temperature between the 20CWP and LIA; (c) differences of surface air temperature between the 20CWP and MWP; (d) time cross section of zonal anomalies in the past millennium (relative to the mean value of 1600–1700). The regions outside the red solid line are significant at the 0.001 confidence level. The regions are not significant over the Weddell Sea in (a) and (b), the Ross Sea in (a) or the high latitude in (c). The typical epochs of the MWP, LIA and 20CWP are on the top left panels. Unit: °C.

North Pacific, and North America were warmer than those of the 20CWP. Hence, the simulated temperature of Europe by the UVic Model may be reasonable, and this phenomenon needs further study.

Figure 4(d) shows the time variation of the zonal anomalies of temperature relative to the mean value of 1600–1700, the coldest period of the LIA. The anomalies in Figure 4(d) were warmer during 1000–1450, with a maximum of 0.6°C during 1100–1260 and a maximum of 0.5°C during 1260–1430 to the north of 30°S. The LIA temperatures were lower globally, with two colder periods during 1600–1700 and 1800–1850 and the coldest year in approximately 1460. The warming of the 20CWP started at 1900 AD. The temperature anomalies at the end of the 20th century reached 1°C over the tropics, 0.8°C over the North Pole, and 0.6°C over the South Pole. In summary, the warming of the MWP was to the north of 30°S, and the cooling of the LIA is global. The warming of the 20CWP was over the tropics and the North and South Poles.

What is the relationship between the variation of the NH and East China during the characteristic periods? Compared with the reconstructed East China temperature [11] (Figure 3(b)) and that of the NH [8] (Figure 2), the temperature anomalies of East China and the NH in the MWP are 0.5°C and 0.3°C, respectively. Hence, the positive anomaly of East China was larger than that of the NH. The temperature anomalies of East China and the NH in the LIA are 0.3°C and 0.2°C, respectively. The negative anomaly of East China in the LIA was also greater than that of the NH. The comparison of the temperature anomaly between the globe and East China is similar to that between the NH and East China. It can be observed in the observational data that temperature anomalies of East China were higher than that of the NH or the globe in the first half of the 20th century [39]. Therefore, the temperature anomalies of East China were higher than that of the NH or the globe in the MWP and the first half of the 20th century and lower than that in the LIA. Figure 5 shows that the simulated temperature anomalies of East China were 0.05–0.1°C higher in the MWP, 0.05°C lower in the LIA, and slightly higher in the first half of the 20th century than that of the globe. The simulated results are consistent with those in the reconstructed and observational data.

4 Contributions of climate forcing factors to the temperature changes of East China in the past millennium

According to the amplitude of the temperature variation, the temperature of East China was divided into several periods to explore their causes and the contributions of the climate forcing factors. Figure 6 shows the temperature of the transient runs minus that of the equilibrium run, which indicates the contributions of climate forcing factors. The red line in Figure 6 represents the contributions to the temperature change of East China under all climate forcing factors. The temperature anomalies under all climate forcing factors reproduce the MWP, LIA, and 20CWP of East China. The durations of the MWP, LIA, and 20CWP are 1000–1430 (not considering the duration of MWP before 1000 AD), 1431–1900, and 1901 to the present, respectively.

The MWP of East China can be divided into three periods, as listed in Table 4. The first period (M1) is 1000–1080. The temperature change of M1 is slightly below normal and is caused by the contributions of solar insolation (blue line) and volcano aerosols (yellow line). The durations of the second (M2) and third (M3) periods of the MWP are 1081–1260 and 1261–1430, respectively. The temperature anomaly of M2 was significantly higher than that of M3. The temperature anomalies of M2 and M3 are consistent with the contribution of solar insolation variation (blue line). Therefore, solar insolation variation is the main cause of the MWP and the shifts from M1 to M2 and from M2 to M3. The shift from the MWP to LIA is also attributed to the decrease in solar insolation in approximately 1430 (Figure 6).

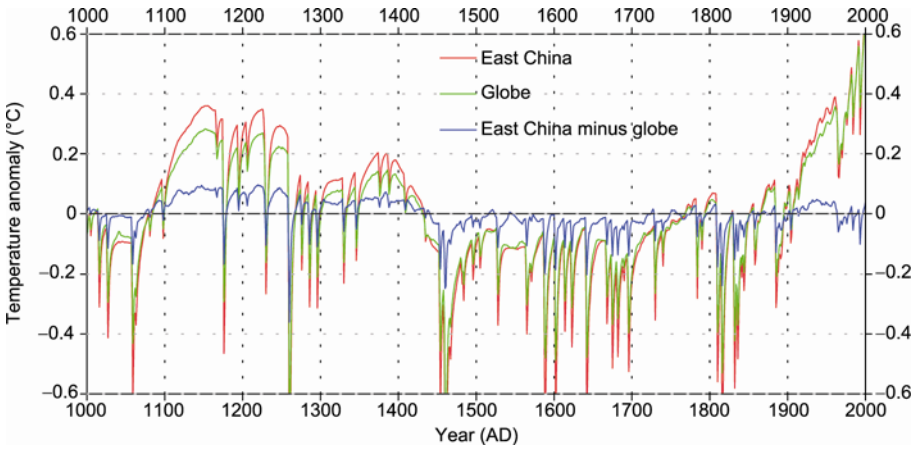

Figure 5 Temperature anomalies of East China and the globe simulated by the UVic Model and its difference. The red and green lines represent the temperature anomalies of East China and the globe relative to the millennial mean values. Unit: °C.

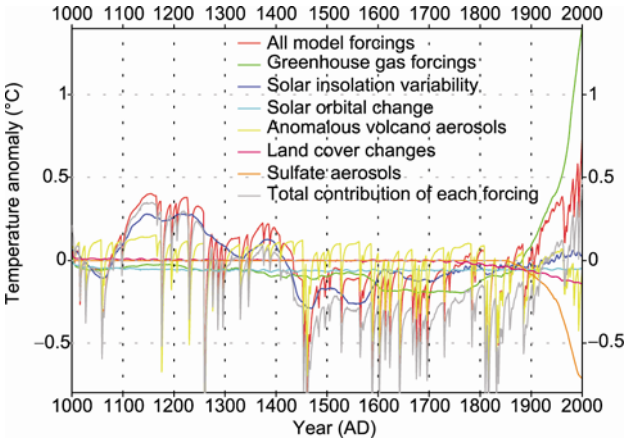

Figure 6 Contributions of climate forcing factors to the temperature variation of East China (transient run minus equilibrium run). The climate forcing factors are greenhouse gases (CO_2 and additional greenhouse gas), solar insolation variability, solar orbit change, anomalous volcano aerosols, land cover changes, and sulfate aerosols. The red and grey lines represent the contributions of all climate forcings and the sum of contributions of individual climate forcings, respectively.

The LIA of East China was divided into four periods (Table 4). The first period (L1, 1431–1585) was induced by weakening of the contribution of solar insolation. The contribution of solar insolation varied from 0.1°C in period M3 of the MWP to –0.2°C in period L1 of the LIA. The second (L2) and third (L3) periods of the LIA are 1586–1700 and 1701–1800, respectively. The shift from L1 to L2 is attributed to the variation of solar insolation, CO_2 and volcano aerosols. It can be observed that the warming contribution of solar insolation (blue line) increased, and the cooling contributions of volcanic eruptions (yellow line) and CO_2 (green line) increased. The temperature anomaly of L2 was lower than that of L1 and L3. The common ground between L2 and L3 is that the cooling effects of solar insolation are small, and the contribution of CO_2 is negative, at approximately –0.15°C. The only difference between L2 and L3 is the frequency of volcanic eruptions. The contribution of volcanic aerosols is approximately –0.2°C in L2 and approximately zero in L3. The fourth period (L4) of the LIA presented cooling in first half of the 19th century and warming in the second half. The variation of L4 is attributed to the contribution from negative to positive of volcanic aerosols; the contributions of the other forcings are all small.

During the 20CWP, the contribution of solar orbit changes, volcanic aerosols and land cover changes are all weakly negative, and that of solar insolation is positive (Figure 6). The warming effects of greenhouse gas were approximately 1.3°C, and the cooling effects of sulfate aerosols were approximately –0.7°C at the end of 20th century. The warming of East China at the end of the 20th century is approximately 0.6°C, which is the sum of the effects of greenhouse gases and sulfate aerosols, consistent with the observed warming value. Therefore, the main causes of warming in the 20CWP are greenhouse gases and sulfate aerosols. The cooling effects of sulfate aerosols played an important role in restraining the climate warming.

5 Contribution of the nonlinear responses among the climate forcing factors to the temperature changes of East China in the past millennium

Figure 6 shows the contribution of all climate forcing factors (red line) is almost higher than the sum of the contributions of individual climate forcing factors (grey line) in the past millennium, indicating that the nonlinear response may exist in the climate system among the climate forcing factors. The net effects of the nonlinear response among the climate forcing factors are positive at end of the 20th century. The following questions then arise: where did the nonlinear responses originate? Were they among the natural climate forcing factors, among the anthropogenic climate forcing factors, or between the natural and anthropogenic climate forcing factors?

We examined the contribution of two groups of climate forcing factors to the temperature changes of East China. The contribution of all climate forcing factors is lower than that of natural climate forcing factors during 1600–1800 and is higher during the others periods (Figure 7). The difference in the contribution of all climate forcing factors minus that of natural climate forcing factors is equal to that of the

Table 4 Main, minor, and transition factors in the air temperature periods of East China in the past millennium[a)]

Temperature in past millennium		Main factors	Minor factors	Transition factors
MWP	M1(1000–1080)	Solar	Volcano	
	M2(1081–1260)	Solar	Volcano	Solar
	M3(1261–1430)	Solar	Volcano	Solar
LIA	L1(1431–1585)	Solar	Volcano	Solar
	L2(1586–1700)	Volcano, GG	–	Solar, GG, Volcano
	L3(1701–1800)	GG	–	Volcano
	L4(1801–1900)	Volcano	–	GG
20CWP	W1(1901–now)	GG, Sulfate	LCC, Solar	GG, Sulfate

a) Main factors stand for the forcing with the main contribution to the temperature change of East China. Minor factors note that the forcing contributed less than that of the main factors. The transition factors indicate that the forcing changed from the previous period to the current period. The line (–) indicates that the contributions of the forcings are all small, except for the contributions of the main forcings.

anthropogenic climate forcing factors. Therefore, there may be no nonlinear responses between the natural and anthropogenic climate forcing factors in the energy moisture balance atmosphere model of the UVic Model. It has been noted that there are nonlinear responses in the climate system under all climate forcing factors. These results indicate that the nonlinear responses may exist among the natural climate forcing factors or the anthropogenic climate forcing factors.

Figure 8 shows that the contribution (red line) of all the natural climate forcing factors was higher than the sum of contributions of the individual factors after 1280 AD. This result indicates that the nonlinear response (blue line) among the natural climate forcing factors has been positive since 1280 AD and that it reached approximately 0.09°C at the end of the 20th century. Likewise, the nonlinear response among the anthropogenic climate forcing factors was 0.18°C at the end of the 20th century. Therefore, the

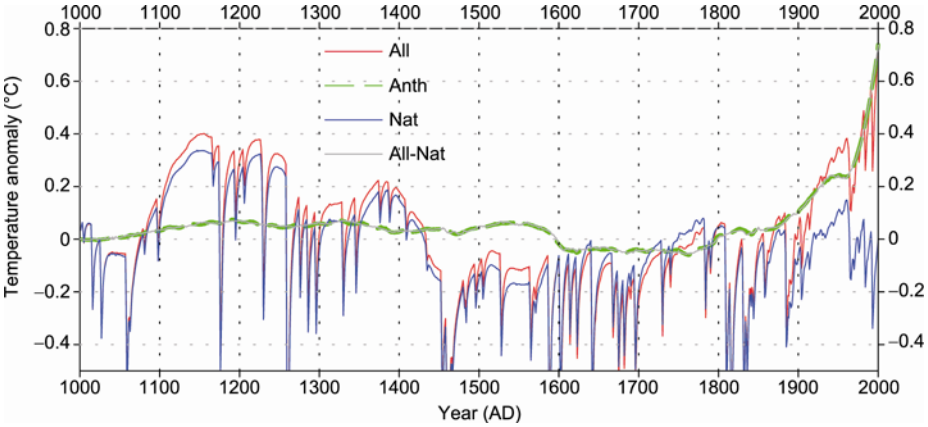

Figure 7 Same as in Figure 6, but showing the contribution of all climate forcing factors (red line) and anthropogenic (green line) and natural climate forcing factors (blue line). The grey line represents the difference in the contribution of all forcing factors minus that of the natural forcing factors (superposition with the green line).

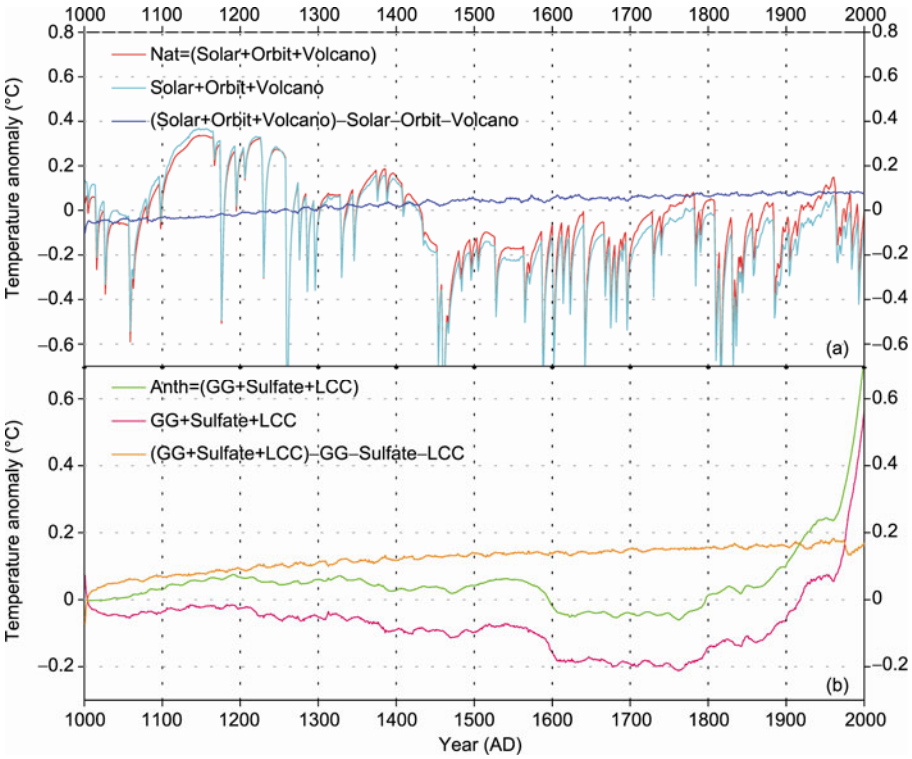

Figure 8 Same as in Figure 6 but showing (a) the contributions of all natural climate forcing factors (red), the sum of contributions of individual natural climate forcing factors (cyan) and its difference (the former minus the latter, blue); (b) the contributions of all anthropogenic climate forcing factors (green), the sum of contributions of individual anthropogenic climate forcing factors (carmine) and the difference between them (the former minus the latter, orange). The contributions of the combined climate forcing factors are shown in parentheses. A climate forcing factor that is not bracketed makes an individual contribution.

nonlinear responses among the natural and anthropogenic climate forcing factors both contributed to the warming of East China at the end of the 20th century. The warming of East China reached approximately 0.6°C at the end of the 20th century under all climate forcings. There is a warming of 0.18°C from the nonlinear response among the anthropogenic climate forcing factors and 0.09°C from the nonlinear response among the natural climate forcing factors, and the sum of which accounted for approximately half of the warming of East China at the end of the 20th century.

We further investigated the nonlinear responses between each group of natural climate forcing factors and between each group of anthropogenic climate forcing factors. The contribution (red line) under the joint forcing of solar insolation and solar orbit change is larger than the sum of their individual contributions (sky-blue line) after 1470 AD (Figure 9(a)). The nonlinear response between the solar insolation and solar orbit change varied from –0.05°C in 1000 AD to 0.02°C at the end of the 20th century. Likewise, the nonlinear responses between the solar orbit change and volcanic aerosols (Figure 9(b)) and between the solar insolation and volcanic aerosols (Figure 9(c)) were 0.18 and –0.02°C at the end of the 20th century, respectively. Half of the sum of the nonlinear responses between the three groups forcings above is equal to 0.09°C, which is consistent with the quantity of the nonlinear responses among the natural climate forcing factors at the end of the 20th century (Figure 8(a)).

Nonlinear responses among the anthropogenic climate forcing factors also contributed warming effects to the temperature anomalies of East China. nonlinear responses between the greenhouse gas and land cover changes (blue, Figure 9(d)) and between the greenhouse gases and anthropogenic sulfate aerosols (sky-blue, Figure 9(e)) both contributed approximately 0.2°C to the warming of East China at the end of the 20th century. However, the nonlinear responses between anthropogenic sulfate aerosols and land cover change are much smaller (Figure 9(f)). The greenhouse gases in the UVic Model are divided into CO_2 and additional greenhouse gas (non-CO_2 greenhouse gas). Furthermore, the nonlinear responses among land cover changes, anthropogenic sulfate aerosols, CO_2, and additional greenhouse gases were also explored. The nonlinear responses between the CO_2 and land cover changes (Figure 9(g)), between CO_2 and anthropogenic sulfate aerosols (Figure 9(h)), between additional greenhouse gas and land cover changes (not shown), and between additional greenhouse gas and anthropogenic sulfate aerosols (not shown) were also smaller at the end of the 20th century. These results indicate that there were no nonlinear responses between either CO_2 or additional greenhouse gases and land cover changes or between that and anthropogenic sulfate aerosols. It can be observed in Figure 9(i) that the nonlinear response between CO_2 and additional greenhouse gases reached –0.2°C at the end of the 20th century. Therefore, only two combinations (CO_2, additional greenhouse gases and anthropogenic sulfate aerosols or CO_2, additional greenhouse gas and land cover changes) could contribute warming effects to the temperature anomalies of East China.

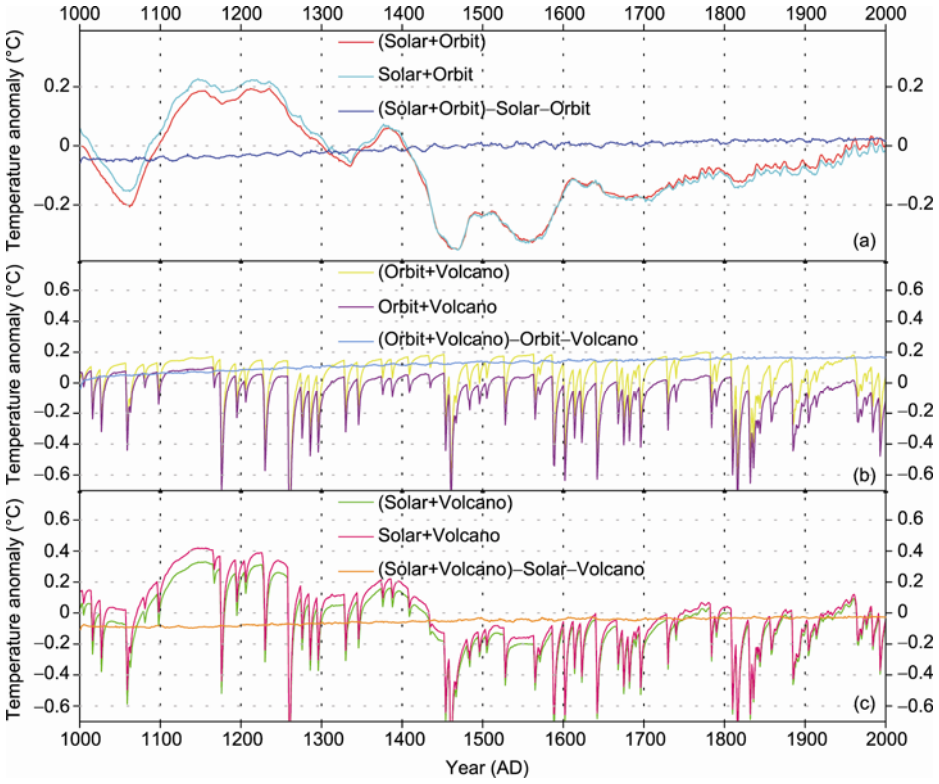

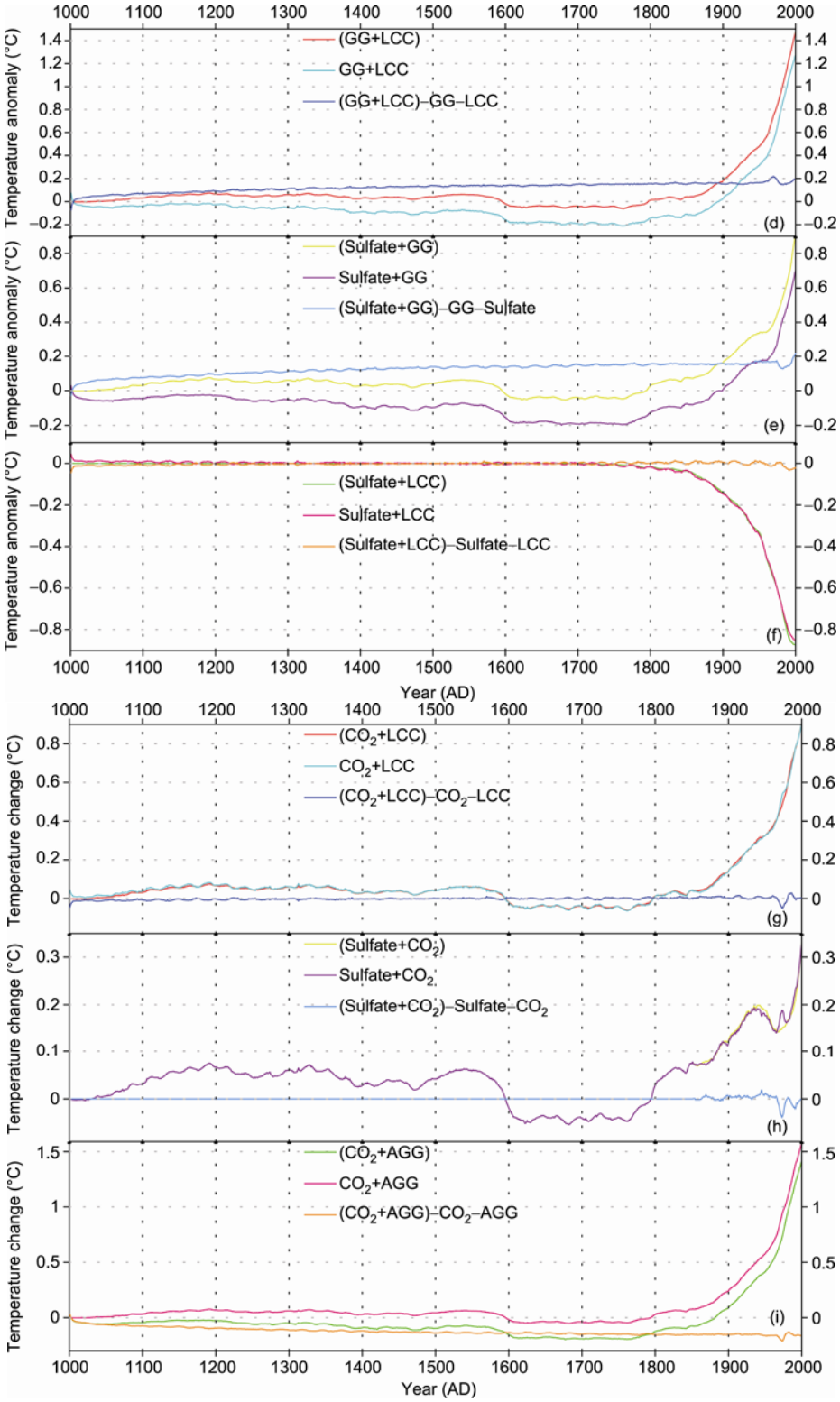

Figure 9 Same as in Figure 8, but showing (a) the joint contributions of solar insolation and solar orbit change (red), the sum of the individual contributions of solar insolation and solar orbit change (cyan), and their difference (the former minus the latter, blue); (b) same as in (a), but showing solar orbit change and volcanic aerosols; (c) same as in (a), but showing solar insolation and volcanic aerosols. (d) the joint contributions of greenhouse gases and land cover changes (red), the sum of the individual contributions of greenhouse gas and land cover change (cyan), and their difference (the former minus the latter, blue); (e) same as in (d), but showing anthropogenic sulfate aerosols and greenhouse gas; (f) same as in (d), but showing anthropogenic sulfate aerosols and land cover changes. (g) the joint contributions of CO_2 and land cover changes (red), the sum of the individual contributions of greenhouse gas and land cover change (cyan), and their difference (the former minus the latter, blue); (h) same as in (g), but showing anthropogenic sulfate aerosols and CO_2; (i) same as in (g), but showing CO_2 and additional greenhouse gases.

In summery, no obvious nonlinear response between the natural and anthropogenic climate forcing factors exists in the atmospheric system of the UVic Model. Nonlinear responses among the natural and anthropogenic climate forcing factors contributed approximately 0.09 and 0.18°C to the temperature anomalies of East China at the end of the 20th century, respectively, the sum of which accounted for approximately half of the warming of East China at that time. The nonlinear response between solar orbit change and volcanic aerosols is 0.18°C, much larger than that between solar orbit change and solar insolation and between solar insolation and volcanic aerosols. The nonlinear response among CO_2, additional greenhouse gas and anthropogenic sulfate aerosols (land cover change), which existed only under the joint effects of the three, reached 0.2°C at the end of the 20th century.

6 Conclusions

The UVic Model was employed to investigate the temperature variation of East China in the past millennium. The UVic Model successfully simulated the temperature variation of the NH and East China. The correlation coefficient between the UVic-simulated NH air temperature and the M08 in the 11-a moving mean time series is 0.76 for 1000–1999 and 0.85 for 1181–1999. The correlation coefficient between the simulated and reconstructed temperatures of East China is 0.5. The UVic Model reproduced the MWP, LIA and 20CWP of East China and the temperature anomalies of East China are warmer during the MWP and the first half of the 20CWP and cooler during the LIA than that of the globe. Therefore, the UVic Model can effectively simulate the temperature variation of East China over the past millennium.

This study employed the UVic Model to explore the contributions of solar insolation variability, solar orbit changes, volcanic aerosols, greenhouse gases, land cover changes and anthropogenic sulfate aerosols to the temperature changes of East China over the past millennium. According to the magnitude of temperature, the temperature of East China was divided into eight periods, three in the MWP, four in the LIA, and one in the 20CWP. The most important forcing during the MWP is solar insolation, followed by volcano aerosols. The shift from the MWP to LIA was also caused by the weakening of solar insolation at that time. The contributions to the LIA originated not only from solar insolation and volcanic aerosols but also from greenhouse gases. The contributions of volcanic aerosols and greenhouse gases were the main causes of the third and fourth periods of the LIA, respectively. Against the warming of greenhouse gases, the cooling effect of anthropogenic sulfate aerosols also played an important role in restraining the warming of East China during the 20th century.

We examined the nonlinear responses among the natural and anthropogenic climate forcing factors, and they contributed approximately 0.09 and 0.18°C to the temperature anomalies of East China at the end of the 20th century, respectively. The contributions of the climate forcing factors reached only 0.33°C at that time. However, no nonlinear response exists between the natural and anthropogenic climate forcing factors in the past millennium. Therefore, approximately half of the warming is attributable to the contribution of nonlinear responses among the climate forcing factors. The physical processes of the nonlinear responses among the climate forcing factors are essential to understanding the cause of climate change in the past millennium, and they need further study.

7 Discussions

We must emphasize the concept of the nonlinear response between the climate forcing factors. For instance, the nonlinear response between solar insolation and land cover changes indicates the difference in the contribution under the combination of solar insolation and land cover changes minus the sum of the individual contributions of solar insolation and land cover changes. For example, assuming that one plus one is equal to 2.5, the nonlinear response is equal to 0.5, which is calculated by following formula (2.5−1−1=0.5). In the transient run of land cover changes, the land cover decreased, and the surface albedo increased; then the solar insolation flux decreased, and the temperature decreased. The variation in solar insolation flux does not represent the nonlinear response between solar insolation and land cover changes but the influences of land cover changes to the variable solar insolation.

This study investigated the response of surface air temperature, an output variable of the atmospheric energy moisture balance of the UVic Model, to climate forcing factors. Hence, the nonlinear responses in this study all originated in the atmospheric system. The climate forcing factors, solar insolation, solar orbit changes, volcanic aerosols, greenhouse gases and anthropogenic sulfate aerosols were all considered as radiation forcings in the UVic Model. The precondition of the nonlinear responses among the climate forcing factors is that the climate forcing factors were coupled as radiation forcings in the energy moisture balance atmosphere model of UVic. Further study is necessary to understand whether the nonlinear responses among the climate forcing factors exist in the complex coupled ocean-atmosphere models.

We thank two anonymous reviewers for their helpful comments, Prof. Wang Shaowu for offering the reconstructed 10-station China temperatures in the past millennium, Prof Liu Jian for offering the ECHO-G simulated temperatures of East China, and NCDC for offering the reconstructed temperatures of China by Yang et al. and Tan et al. This work was supported by the Major Project of National Natural Science Foundation of China (Grant No. 40890052), National Basic Research Progam of China

(Grant No. 2007CB815901), National Natural Science Foundation of China (Grant No. 40805036) and the Basic Research Fund of CAMS.

1 IPCC. The Physical Science Basis. Cambridge: Cambridge University Press, 2007. 996
2 Zhou T, Man W M, Zhang J. Progress in numerical simulations of the climate over the last millennium (in Chinese). Adv Earth Sci, 2009, 24: 469–476
3 Mann M E, Bradley R S, Hughes M K. Global-scale temperature patterns and climate forcing over the past six centuries. Nature, 1998, 392: 779–782
4 Mann M E, Bradley R S, Hughes M K. Northern Hemi sphere temperatures during the past millennium: inferences, uncertainties and limitations. Geophys Res Letts, 1999, 26: 759–762
5 Soon W, Baliunas S, Idso C. Reconstructing climatic and environmental changes of the past 1000 years: Reappraisal. Energy Environ, 2003, 4: 233–296
6 Jones P D, Mann M E. Climate over the past millennia. Rev Geophys, 2004, 42: RG2002
7 Mann M E, Jones P D. Global surface temperatures over the past two millennia. Geophys Res Lett, 2003, 30: 1820
8 Mann M E, Zhang Z, Hughes M K, et al. Proxy-based reconstructions of hemispheric and global surface temperature variations over the past two millennia. Proc Natl Acad Sci USA, 2008, 105, doi: 10.1073/pnas.0805721105
9 Wang S W, Luo Y, Zhao Z C, et al. Debate still continues about temperature changes during the last millennium (in Chinese). Adv Clim Change Res, 2005, 2: 72–75
10 Wang S W, Xie Z H, Cai J N, et al. Study of the global mean temperature variation during the last millennium. Prog Nat Sci, 2002, 12: 1145–1149
11 Wang S W, Wen X Y, Luo Y, et al. Reconstruction of temperature series in China during the last millennium. Chin Sci Bull, 2007, 52: 958–964
12 Yang B, Braeuning A, Johnson K R, et al. General characteristics of temperature variation in China during the last two millennia. Geophys Res Lett, 2002, doi: 10.1029/2001GL014485
13 Ge Q J, Zheng X, Fang X Q, et al. Winter half-year temperature reconstruction for the middle and lower reaches of the Yellow River and Yangtze River, China, during the past 2000 years. Holocene, 2003, 13: 933–940
14 Tan M, Liu T S, Hou J, et al. Cyclic rapid warming on centennial-scale revealed by a 2650-year stalagmite record of warm season temperature. Geophys Res Lett, 2003, 1617, doi: 10.1029/2003GL017352
15 Shao X M, Huang L, Liu H B, et al. Reconstruction of precipitation variation from tree rings in recent 1000 years in Delingha, Qinghai. Sci China Ser D-Earth Sci, 2004, 34: 939–949
16 Yao T D, Yang Z H, Huang C L, et al. A continuous climatic and environmental records during recent 2 ka: Preliminary study of Guliya ice core in recent 2000 years. Chin Sci Bull, 1996, 41: 1103–1106
17 Wang S W, Luo Y, Wen X Y, et al. Latest advances in studies of the global temperature variations for the last millennium (in Chinese). Adv Clim Change Res, 2007, 3: 14–19
18 Chu Z Y, Ren G Y. An overview of the research on temperature variability of the last 1000 years (in Chinese). Clim Environ Res, 2005, 10: 818–825
19 Zheng J Y, Wang S W. Assessment on climate change in China for the last 2000 years (in Chinese). Acta Geogr Sin, 2005, 60: 21–31
20 Liu J, Storch H V, Chen X, et al. Long-time modeling experiment on global climate change for the last millennium (in Chinese). Adv Earth Sci, 2005, 20: 561–567
21 Liu J, Storch H V, Chen X, et al. Simulated and reconstructed winter temperature in the eastern China during the last millennium. Chin Sci Bull, 2005, 50: 2251–2255
22 Zhang J, Zhou T J, Man W M, et al. The transient simulation of little ice age by LASG/IAP climate system model FGOALS_gl (in Chinese). Quat Sci, 2009, 29: 1125–1134
23 Man W M, Zhou T J, Zhang J, et al. The equilibrium response of LASG/ IAP climate system model to prescribed external forcing during the little ice age (in Chinese). J Atmos Sci, 2010, 34: 914–924
24 Zhou T, Yu R. Twentieth century surface air temperature over China and the globe simulated by coupled climate models. J Clim, 2006, 19: 5843–5858
25 Zhang R, Li L, Guo Q C, et al. The development and application of climate model in paleoclimate simulation (in Chinese). Arid Zone Res, 2007, 24: 704–711
26 Weaver A J, Eby M, Wiebe E C, et al. The UVic Earth System Climate Model: Model description, climatology, and applications to past, present and future climates. Atmos-Ocean, 2001, 39: 1–68
27 Matthews H D, Weaver A J, Meissner K J, et al. Natural and anthropogenic climate change: Incorporating historical land cover change, vegetation dynamics and the global carbon cycle. Clim Dyn, 2004, 22: 461–479
28 Meissner K J, Eby M, Weaver A J, et al. CO_2 threshold for millennial-scale oscillations in the climate system: implications for global warming scenarios. Clim Dyn, 2008, 30: 161–174
29 Rennermalm A K, Wood E F, Weaver A J, et al. Relative sensitivity of the Atlantic meridional overturning circulation to river discharge into Hudson Bay and the Arctic Ocean. J Geophys Res, 2007, 112: G04S48
30 Bard E, Raisbeck G, Yiou F, et al. Solar irradiance during the last 1200 years based on cosmogenic nuclides. Tellus B, 2000, 52: 985–992
31 Krivova N A, Balmaceda L, Solanki S K. Reconstruction of solar total irradiance since 1700 from the surface magnetic flux. Astron Astrophys, 2007, 467: 335–346
32 Crowley J T. Causes of climate change over the past 1000 years. Science, 2000, 289: 270–277
33 Sato M, Hansen J E, McCormick M P, et al. Stratospheric aerosol optical depths, 1850–1990. J. Geophys Res, 1993, 98: 22987–22994
34 Indermühle A, Monnin E, Stauffer B, et al. Atmospheric CO_2 concentration from 60 to 20 Ka BP from the Taylor Dome Ice Core, Antarctica. Geophys Res Lett, 2000, 27: 735–738
35 Bauer E, Claussen M, Brovkin V, et al. Assessing climate forcings of the Earth system for the past millennium. Geophys Res Lett, 2003, 30: 1276
36 Chen W Y. Fluctuation in Northern Hemisphere 700 mb height field associated with Southern Oscillation. Mon Weather Rev, 1982, 110: 808–832
37 Crowley T J, Lowery T S. How warm was the medieval warm period? Ambio, 2000, 29: 51–54
38 Mann M E, Zhang Z, Rutherford S, et al. Global signatures and dynamical origins of the Little Ice Age and medieval climate anomaly. Science, 2009, 326: 1260
39 Wang S W, Luo Y, Zhao Z C, et al. Debate about climate warming. Prog Nat Sci, 2005, 15: 917–622